Three-dimensional inversion of large-scale EarthScope magnetotelluric data based on the integral equation method: Geoelectrical imaging of the Yellowstone conductive mantle plume

Michael S. Zhdanov,[1] Robert B. Smith,[1] Alexander Gribenko,[1] Martin Cuma,[1] and Marie Green[1]

Received 6 February 2011; revised 22 March 2011; accepted 28 March 2011; published 28 April 2011.

[1] Interpretation of the EarthScope MT (magnetotelluric) data requires the development of a large-scale inversion method which can address two common problems of 3D MT inversion: computational time and memory requirements. We have developed an efficient method of 3D MT inversion based on an IE (integral equation) formulation of the MT forward modeling problem and a receiver footprint approach, implemented as a massively parallel algorithm. This method is applied to the MT data collected in the western United States as a part of the EarthScope project. As a result, we present one of the first 3D geoelectrical images of the upper mantle beneath Yellowstone revealed by this large-scale 3D inversion of the EarthScope MT data. These images show a highly conductive body associated with the tomographically imaged mantle plume-like layer of hot material rising from the upper mantle toward the Yellowstone volcano. The conductive body identified in these images is west-dipping in a similar way to a P-wave low-velocity body. **Citation:** Zhdanov, M. S., R. B. Smith, A. Gribenko, M. Cuma, and M. Green (2011), Three-dimensional inversion of large-scale EarthScope magnetotelluric data based on the integral equation method: Geoelectrical imaging of the Yellowstone conductive mantle plume, *Geophys. Res. Lett.*, *38*, L08307, doi:10.1029/2011GL046953.

1. Introduction

[2] EarthScope is a National Science Foundation program designed to explore the structure and evolution of the North American continent, and to further understand the processes controlling earthquakes and volcanoes. A major part of the EarthScope project is the USArray of seismic, magnetotelluric, and geodetic instruments that are being deployed over the current decade across the entire continental United States. This transportable array of geophysical instruments provides an unparalleled means to study the crust and mantle geology of the United States through seismology and magnetotelluric data. EMScope is the magnetotelluric component of the USArray program, managed by Oregon State University on behalf of Incorporated Research Institutions for Seismology (IRIS). EMScope comprises long-period investigations at hundreds of sites in the continental United States, in addition to a number of long-period backbone stations. By mid-2010, MT data had been collected at about 250 stations located throughout Oregon, Washington, Idaho, northern California, most of Wyoming and Montana, and large sections of Nevada. The preliminary results of interpretation of the EarthScope MT data collected over Washington, Oregon, Montana, and Idaho were presented in the papers by *Patro and Egbert* [2008] and *Zhdanov et al.* [2010]. In the current paper we focus our attention on more recent EarthScope MT dataset collected in Montana, Idaho, and Wyoming.

[3] The unique geological setting of the western United States including plate boundary transform faulting, subduction, intraplate extension of the Basin-Range and the active Yellowstone hotspot, is very important both for the study of its geodynamical history and for understanding the physical processes controlling earthquakes and volcanic eruptions [*Bishop*, 2003]. It is a tectonically active region with the subducting Juan de Fuca plate and volcanically important from the effects of the Juan de Fuca/Gorda plates moving over a mantle plume currently located beneath Yellowstone. For such a complex region, definitive structural interpretations based purely on seismological observations are not complete for a more comprehensive study of the deep earth interior without including its electrical structure. Conductivity in the subsurface plays a significant role in determining tectonic activities principally because of its sensitivity to temperature, the presence of interstitial fluids, melts, volatiles, and bulk composition.

[4] The magnetotelluric (MT) method makes use of natural variations in electromagnetic fields to determine the electrical structure of the Earth. In recent years, the MT method has undergone rapid development. Significant improvements have been made both in MT data acquisition systems and in the quality of processing and analyzing these data. Modern MT surveys provide high quality data from an array of densely distributed MT stations, which contain unique information about the geoelectrical structure of geological formations. In order to extract this information from the EarthScope MT data collected at hundreds of sites in the northwestern continental United States, one should employ a very large-scale inversion of the MT data, which would allow the researcher to reconstruct the spatial distribution of the electrical conductivity in the area of several hundred square km and at a depth of a few hundred km. In order to address this problem, we have developed massively parallel 3D MT inversion algorithms and software based on the rigorous integral equation (IE) method for forward modeling and on the regularization theory for inversion, which considerably reduces the computational resources needed to invert the

[1]Department of Geology and Geophysics, University of Utah, Salt Lake City, Utah, USA.

0094-8276/11/2011GL046953

large volumes of data covering vast areas. We apply the developed 3D inversion method to MT data collected in the western United States as a part of the EarthScope project.

2. Large-Scale Massively Parallel Inversion of MT Data

[5] The development of a large-scale, three-dimensional (3D) MT inversion method represents a very challenging numerical and practical problem. The reasons are twofold. First, 3D forward modeling is a highly complicated and time-consuming computational problem itself, especially for large-scale geoelectrical models. Second, the inversion of MT data is an unstable and nonunique problem, meaning that it is an ill-posed problem. One should use regularization methods and physical constraints to obtain a stable and geologically meaningful solution to an MT inverse problem.

[6] In developing our large-scale MT inversion algorithm, we use the integral equation (IE) method as the main engine for forward modeling. The IE method in numerical dressing is reduced to a linear system of equations,

$$(\mathbf{I} - \mathbf{Gm})\mathbf{E} = \mathbf{E}b, \tag{1}$$

where $\mathbf{m}$ is a matrix of the conductivity of the model, $\mathbf{I}$ is the identity matrix, $\mathbf{G}$ is the matrix of the volume-integrated Green's tensors for the background conductivity model, $\mathbf{E}$ and $\mathbf{E}b$ are the vectors of the total and background electric fields, respectively. Following *Hursán and Zhdanov* [2002] and *Zhdanov* [2009], we precondition equation (1) with contraction operators to improve the conditioning of the matrix system, and we also exploit the Toeplitz structure of the matrix system (1), meaning that we can perform multiplications of the translationally invariant horizontal components of $\mathbf{G}$ without needing to store its full size.

[7] There are several advantages in using the IE method in the MT data inversion in comparison with the more traditional finite-difference (FD) approach. First, IE forward modeling requires the calculation of Green's tensors for the background conductivity model. These tensors can be precomputed only once and saved for multiple uses on every iteration of inversion, which materially speeds up the computation of the predicted data on each iteration significantly. Second, the same precomputed Green's tensors can be readily used for Fréchet derivative calculations, which is another important element of inversion. Finally, IE forward modeling and inversion requires the discretization of the domain of inversion only, while in the framework of the FD method one has to discretize the entire modeling domain, which includes not only the area of investigation but an additional domain surrounding this area. Moreover, we will show below that one can exploit the fact that the area of the "footprint" of an MT station is significantly smaller than the area of an entire MT survey, which would allow us to develop a large-scale 3D inversion algorithm based on the IE method, which uses an MT station footprint approach.

[8] To solve the ill-posed MT inverse problem, we use Tikhonov regularization, which is based on minimization of the following parametric functional [*Tikhonov and Arsenin*, 1977; *Zhdanov*, 2002]:

$$P(\mathbf{m}) = f(\mathbf{m}) + \alpha S(\mathbf{m}) = \min, \tag{2}$$

where $f(\mathbf{m})$ is the misfit functional between the predicted data, $A(\mathbf{m})$, and the observed data $\mathbf{d}$; A is the nonlinear forward operator symbolizing the governing equations of the MT forward modeling problem; $S(\mathbf{m})$ is a stabilizing functional; and α is a regularization parameter.

[9] We solve this minimization problem using the reweighted regularized conjugate-gradient (RRCG) method with adaptive regularization parameter selection [*Zhdanov*, 2002]. The RRCG algorithm is based on iterative updates of the conductivity model $\mathbf{m}(n)$ so as to minimize the functional $P(\mathbf{m})$:

$$\mathbf{m}(n+1) = \mathbf{m}(n) + k(n)F^* \mathbf{r}(n), \tag{3}$$

where n is the iteration number, $k(n)$ is a step length, $\mathbf{r}(n)$ is the vector of residual errors, and F^* is the conjugate transpose of the Fréchet derivative matrix of sensitivities at the nth iteration. It is well known that there exist different methods of computing the gradient $F^* \mathbf{r}(n)$ [e.g., *Zhdanov*, 2002]. Some methods could be based on direct calculations of the Fréchet derivative matrix F using different fast but accurate approximations (e.g., quasi-analytical approximation). Another methods use a solution of the adjoint problem without direct calculations of F. However, under any scenario computing the gradient requires the most calculations in the inversion not only in terms of the computation time, but also in terms of the amount of computer memory required for its storage. With large amounts of data and vast inversion regions, the computer memory requirements may become prohibitive. To reduce the storage requirements, we use a footprint approach in our MT inversion [*Zhdanov et al.*, 2010; *Cox et al.*, 2010].

[10] In the framework of the footprint approach, for a given receiver we compute and store the Fréchet derivative and/or gradient $F^*\mathbf{r}(n)$ inside the inversion cells within a predetermined horizontal distance from this receiver only, i.e., within a footprint. Thus, Fréchet derivatives for an MT station and/or corresponding gradient can be computed and stored for regions much smaller than the entire inversion domain only, resulting in dramatic reduction of the computer memory requirements.

[11] The footprint size is determined based on the rate of sensitivity attenuation of the MT data. As an example, we consider a model of a 75 Ohm-m half-space to demonstrate the limited spatial extent of MT station sensitivity. It is obvious that the sensitivity of the MT data to the local variation of the model conductivity at a given point decreases with the distance. Figure 1 (top) shows the percentage of the total MT response from within a square footprint of varying sizes, calculated as L2 norm of the principal MT impedances at different frequencies in the observation point located in the center of the square footprint. As we would expect, Figure 1 (top) demonstrates that the higher frequencies have a smaller footprint with almost 95% of their response coming from within a 100 km footprint, while for the lower frequencies the same percentage of the response comes from within a 450 km footprint. We apply the footprint approach for the Fréchet derivative and/or corresponding gradient calculation and not for the computations of the predicted field. By using all of the cells in the forward modeling computations, we ensure an accurate result for the calculations of the predicted fields in the receivers. Our large-scale 3D MT data inversion is implemented as massively parallel software with two levels

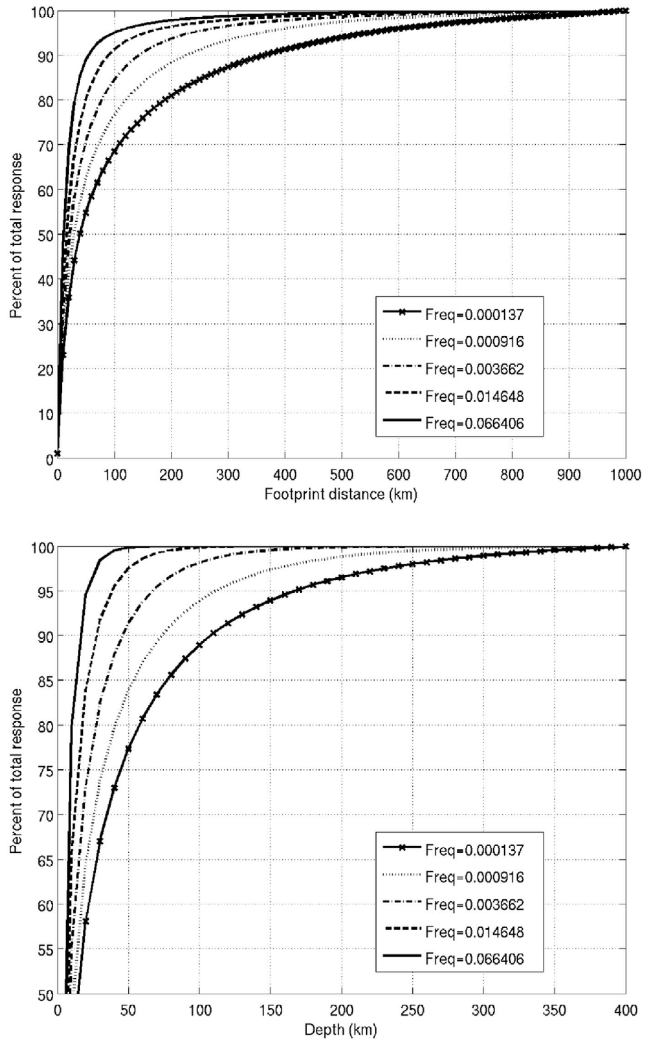

Figure 1. (top) Percentage of the total MT response within a square footprint, calculated as L2 norm of the principal MT impedances at different frequencies in the observation point located in the center of the square footprint. The length of one side of the square is given on the abscissa, and the percent of this response normalized by the total response of the entire model is given on the ordinate. (bottom) Percentage of the total MT response within a given depth, calculated as L2 norm of the principal MT impedances at 28 MT stations located in the Yellowstone hotspot area. The depth of the inversion domain with anomalous conductivity is given on the abscissa, and the percent of this response normalized by a total response of the model is given on the ordinate.

of parallelization; the higher level parallelizes over the frequencies of the MT field, the lower level over the horizontal layers of the discretization grid and field components.

3. Inversion of EarthScope MT Data

[12] Figure 2 presents a map of the western United States with the locations of the EarthScope MT stations collected in 2009 in Montana, Idaho, and Wyoming (shown by red dots). It is important to note that the Yellowstone hotspot is located in the center of this area. Yellowstone is an example of a continental hotspot that is located 1600 km east of the western North American plate boundary. While most of Earth's volcanism is associated with plate boundaries, including mid-ocean ridges and subduction zones, the Yellowstone hotspot occurs within a continental plate and resulted from a mantle plume interacting with the overriding North America plate [e.g., *Schutt et al.*, 2008; *Smith et al.*, 2009; *Obrebski et al.*, 2010; *Schmandt and Humphreys*, 2010]. In traditional geologic thinking, such plumes ascend vertically from the core-mantle boundary to the base of the lithosphere [e.g., *Morgan*, 1971]. New models, however, predict that plumes can rise buoyantly upward along curved paths, tilted by the directions of convective mantle flow, and may not necessarily have a core-mantle boundary source [e.g., *Steinberger et al.*, 2004]. Thus, hotspots are not necessarily fixed, and horizontal mantle flow can deflect and tilt a plume. Seismic tomography has revealed complex multi-scale heterogeneity of the western United States upper mantle, closely related to tectonic and magmatic activities [e.g., *Schutt et al.*, 2008; *Schmandt and Humphreys*, 2010]. *Yuan and Dueker* [2005], *Waite et al.* [2006], and *Smith et al.* [2009] presented the first P-wave tomographic images of the upper mantle beneath the Yellowstone hotspot area. These data revealed a well defined low-velocity body from ~80 to 250 km directly under the Yellowstone caldera extending from 80 to 200 km beneath the eastern Snake River Plain, and a 60° west-tilted, low-velocity body from 200 to ~600 km as a plume of partial melt that extends upward from the bottom of the mantle transition zone.

[13] In the first stage of our analysis of the Yellowstone-focused MT array, we have applied the above inversion method to the principal MT impedances observed at 24 frequencies ranging from 0.0001 to 0.0664 Hz from 115 MT stations distributed across Montana, Idaho, and Wyoming, shown by the red dots in Figure 2. In this case, the inversion domain was spanned in the X (geographic E–W), Y (geographic N–S), and Z (vertical downward) directions extending 900 km, 850 km, and 500 km, respectively. We used discretization cells with a horizontal size of 5 km by 5 km, and vertical cell sizes starting from 1 km at the top and increasing with depth logarithmically. The total number of cells in the inversion domain was $180 \times 170 \times 64 = 1{,}958{,}400$. The initial model was selected as a uniform 75 Ohm-m half-space.

[14] A well known problem in 3D MT data inversion is the removal of static shift, which is due to the presence of relatively small-scale, near-surface inhomogeneities. We have reduced the static shift effect by normalizing the observed MT impedances with their absolute values, which effectively resulted in the phase inversion of the impedances. It is well known that the phases are less sensitive to the galvanic distortions, caused by near-surface inhomogeneities. Figure 3 shows the 3D geoelectrical model obtained by the inversion of the EarthScope MT data using a 450 km footprint. The inversions were run until the L2 norm of the residuals between the observed and theoretically predicted MT data, normalized by the L2 norm of the observed data, decreased to about 10%. Note that the misfit calculations were based on the real and imaginary parts of the principal MT impedances. The distinguished feature of the inverse geoelectrical model is a large conductive body, which we interpret to be associated with a plume-like structure of hot conductive material in the upper mantle.

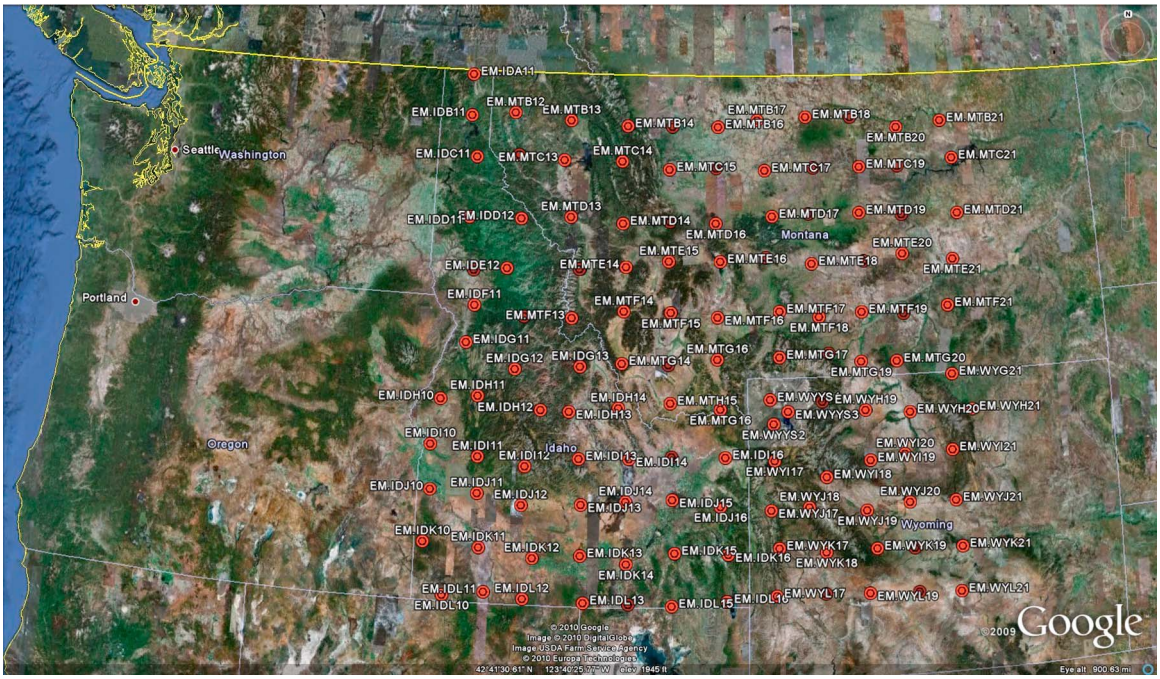

Figure 2. Map of the western United States showing the locations of the EarthScope MT stations collected across the Yellowstone hotspot region of Montana, Idaho, and Wyoming (shown by red dots).

[15] In the next stage of our analysis we focused our attention on the area surrounding Yellowstone National Park. We selected 28 MT stations located relatively close to Yellowstone. In this case, the inversion domain was spanned in the X (geographic E–W), Y (geographic N–S), and Z (vertical downward) direction extending 448 km, 400 km, and 500 km, respectively. We used discretization cells with a horizontal size of 4 km by 4 km, and relatively fine vertical discretization

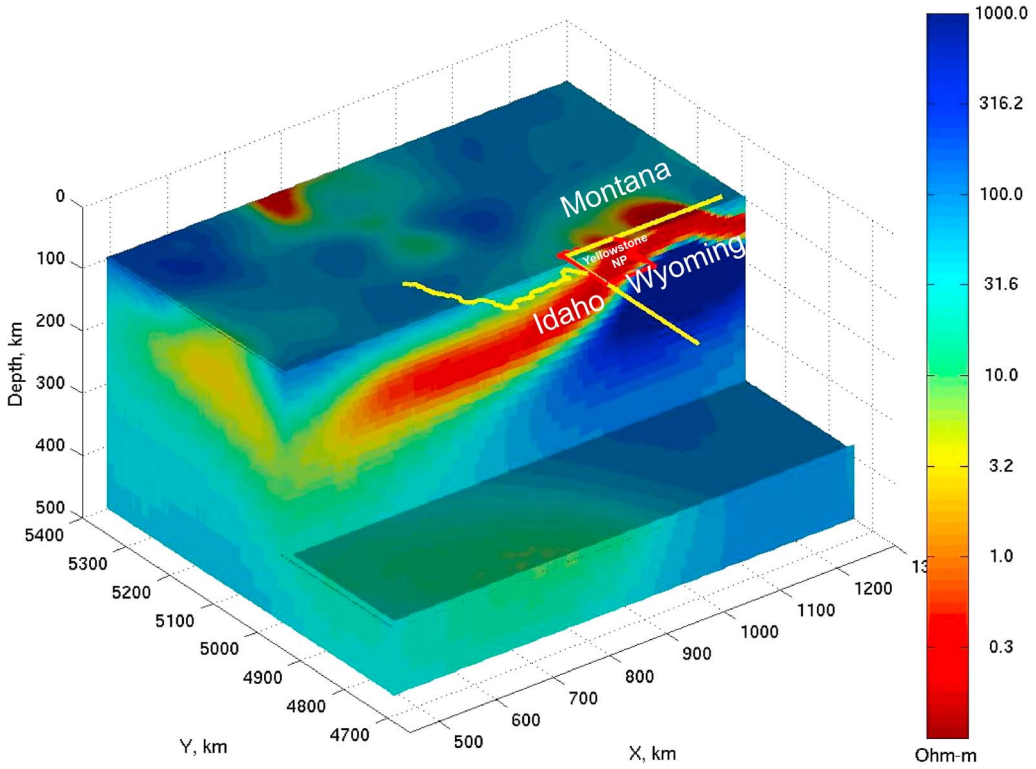

Figure 3. Three-dimensional geoelectrical resistivity model obtained by the inversion of the MT data from 115 MT stations distributed across Montana, Idaho, and Wyoming, shown in Figure 2. The vertical section is drawn across Yellowstone Park, while the horizontal section is drawn at a depth of 400 km.

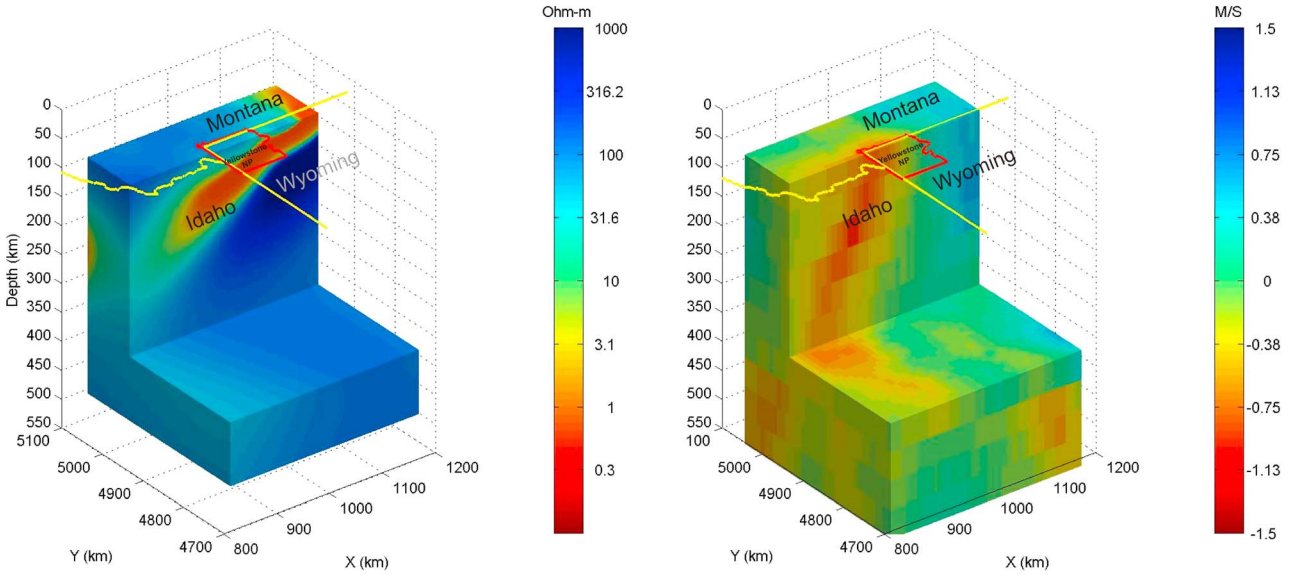

Figure 4. (left) A 3D geoelectrical resistivity model obtained by inversion of the MT data over the Yellowstone hotspot area. (right) A P-wave seismic tomography image of Yellowstone represented by a rising column of partly molten rock originating in the mantle transition zone. The vertical sections in both images are drawn across Yellowstone Park, while the horizontal sections are drawn at a depth of 400 km.

with vertical cell sizes starting at 1 km near the surface and increasing logarithmically to the bottom. The total number of cells in the inversion domain was 112 × 100 × 128 = 1,433,600. The initial model was selected, as above, as a 75 Ohm-m half-space, and we imposed an upper limit of 5 S/m on the inverse conductivity. The inversion was run until the L2 norm of the residuals decreased to 10%. Figure 4 (left) presents a spatial view of a 3D geoelectrical model obtained by the inversion of the EarthScope MT data over the Yellowstone National Park area.

[16] One can clearly see a plume-like structure of conductive hot mantle rising from the mantle transition zone at a depth of ~300 km. Remarkably, our inversion images indicate high conductivity of this structure (a few S/m). In order to verify this result, we ran several inversion scenarios with different upper limits on the conductivity: 0.5 S/m, 1 S/m, 3 S/m, and 5 S/m, respectively. Note that, different inversion results indicate that for the higher conductivity of the plume we have the better convergence rate of the inversion.

[17] All these inversions produced images of the conductive plume-like structure in the upper mantle with a similar shape but different conductivities, reflecting the imposed upper bounds. This result is justified because the MT response saturates as the conductivity of a body becomes greater than 20–50 times that of the background value. In the Yellowstone area, bulk conductivities of the plume layer are almost 100 times the background conductivities and, for the skin depths of interest, the MT response is totally governed by the concentration of electric currents in the conductive structure. It is easy to demonstrate, for example, that for a 50 km thick conductive layer buried 150 km deep in a 75 ohm-m background (somewhat similar to the Yellowstone conductive plume-like layer), the difference between conductivities of 1 S/m and 5 S/m for the conductive layer yields no appreciable differences in the MT response; hence the response has saturated. The difficulty in resolving the true conductivity at 150–250 km depth logically follows from this as well. Based on this numerical study we can cautiously conclude that the realistic number of the conductivity of the plume-like structure, revealed by the MT data, is on an order of a few S/m. This conductivity level is comparable to the conductivity of the silicate melts found in the lab experiment [*Pommier et al.*, 2008; *Pommier and Le Trong*, 2011], and it can logically be explained by a combination of high temperature partial melt, and the presence of highly saline fluids associated with the magmatic processes. For example, one can use the Hashin-Shtrikman upper bound to calculate the bulk resistivity of the two-phase mixture formed by high-conductivity liquid phase surrounding by a less conductive rock material [*Hashin and Shtrikman*, 1962]. We suggest that the high conductive body revealed by MT inversion represents a body rich in partially melted material mixed with the highly saline interstitial fluids. A similar result indicating the presence of very high conductive zones beneath the Yellowstone volcanic field and its three Quaternary giant calderas with the conductivity up to a few S/m was reported by *Kelbert et al.* [2010]. However, a detailed evaluation of electrical properties of the silicate melts at the depth of several hundred km is beyond the scope of our paper. More research is needed to better understand this phenomenon.

[18] For a comparison, we present in Figure 4 (right) the same 3D cut-away view of the P-wave velocity anomaly model, produced by *Smith et al.* [2009]. One can observe remarkable similarity between the images of the Yellowstone plume produced independently by seismic tomography and those produced by 3D MT inversion. The conductive body identified in the geoelectrical image (Figure 4, left) is west-dipping in a similar way to the low-velocity body shown in the P-wave seismic tomography image (Figure 4, right). Taking into account the different physical natures of the seismic velocity anomaly and the conductivity anomaly, one should not expect that these two images would coincide

completely. However, we observe that the two images associated with the mantle "plume" – one from the seismic data and the other from the MT data – are similar to each other, which is a good indication that these two images manifest the similar interacting large-scale velocity-compositional structure in the upper mantle beneath Yellowstone. The observed differences in the geophysical images should be expected considering the different physical nature of seismic and MT data, different survey configurations, and different depth resolution of the two geophysical techniques.

[19] We note that, the depth resolution of the MT data at below 300 km is very poor compared to the seismic images because of the rapid attenuation of the diffusive EM field with the depth. We have conducted an analysis of the sensitivity of the MT data to the conductivity anomalies at different depths for a given inverse model. Figure 1 (bottom) represents the percentage of the total MT response within a given depth of the inversion domain with anomalous conductivity, calculated as L2 norm of the principal MT impedances at 28 MT stations located in the Yellowstone hotspot area. About 98% of the total response comes from within a 300 km depth. This limit can be explained by the absence of visible anomalies below 300 km in the inverse images (see Figure 4, left). Nevertheless, the general character of the geoelectrical and seismic images has a remarkable similarity that indicates the presence of the mantle plume associated with the hot material rising from the mantle toward the Yellowstone volcano.

[20] In recent publications, *Waite et al.* [2005, 2006], *Schutt and Dueker* [2008], *Smith et al.* [2009], and *Xue and Allen* [2010], have interpreted this low-velocity body as a high-temperature plume layer with excess temperatures of up to 300 K. The geoelectrical image, obtained as a result of large-scale MT inversion, is consistent with this model as well.

4. Conclusion

[21] In conclusion, we specifically note that new studies of the Yellowstone plume include analyses of seismic wave attenuation for P- and S-waves [e.g., *Adams and Humphreys*, 2010]. They reveal relatively high attenuation of the mantle volume, which is seismically imaged as the Yellowstone plume interpreted to reflect a partially molten plume in which water is partitioned into the melt and surrounded by a cooler and wetter mantle. A notable attenuation decrease at 200−250 km is considered by *Adams and Humphreys* [2010] as evidence that the plume is melting above this depth. This corresponds well to the area of high conductivity above 250 km in the geoelectrical model shown in Figure 4.

[22] Thus, the developed massively parallel 3D MT inversion with a receiver footprint makes it practical to invert continental-scale MT data acquired as a part of the EarthScope project. Our 3D resistivity model of the upper mantle under Yellowstone provides an independent confirmation based on MT data of the presence of a plume-like body of hot conductive material rising from the upper mantle towards the Yellowstone volcano. Note that our new findings do not provide any information on the chances of future volcanic eruption.

[23] **Acknowledgments.** We wish to acknowledge the support of the University of Utah Consortium for Electromagnetic Modeling and Inversion (CEMI). The MT data were acquired by the Incorporated Research Institutions for Seismology (IRIS) as part of the operation of the USArray. Data used in this study were made available through Earth-Scope (www.earthscope.org; EAR-0323309), supported by the National Science Foundation. We also acknowledge allocation of computer time provided by the University of Utah's Center for High Performance Computing (CHPC). The authors acknowledge TechnoImaging for support of this research. We are thankful to Adam Schultz for his useful comments and suggestions, which helped to improve the manuscript.

[24] The Editor thanks Adam Schultz and an anonymous reviewer for their assistance in evaluating this paper.

References

Adams, D. C., and E. D. Humphreys (2010), New constraints on the properties of the Yellowstone mantle plume from P and S-wave attenuation tomography, *J. Geophys. Res.*, *115*, B12311, doi:10.1029/2009JB006864.

Bishop, E. M. (2003), *In Search of Ancient Oregon: A Geological and Natural History*, Timber, Portland, Oregon.

Cox, L. H., G. A. Wilson, and M. S. Zhdanov (2010), 3D inversion of airborne electromagnetic data using a moving footprint, *Explor. Geophys.*, *41*, 250–259, doi:10.1071/EG10003.

Hashin, Z., and S. Shtrikman (1962), On some variational principles in anisotropic and nonhomogeneous elasticity, *J. Mech. Phys. Solids*, *10*, 335–342, doi:10.1016/0022-5096(62)90004-2.

Hursán, G., and M. S. Zhdanov (2002), Contraction integral equation method in three-dimensional electromagnetic modeling, *Radio Sci.*, *37*(6), 1089, doi:10.1029/2001RS002513.

Kelbert, A., G. D. Egbert, C. D. Degroot-Hedlin, and N. Meqbel (2010), Properties of the magmatic system that feeds Yellowstone inferred from 3-D electrical conductivity model, Abstract DI23A-1968 presented at 2010 Fall Meeting, AGU, San Francisco, Calif., 13–17 Dec.

Morgan, W. J. (1971), Convection plumes in the lower mantle, *Nature*, *230*, 42–43, doi:10.1038/230042a0.

Obrebski, M., R. M. Allen, M. Xue, and S. H. Hung (2010), Slab-plume interaction beneath the Pacific Northwest, *Geophys. Res. Lett.*, *37*, L14305, doi:10.1029/2010GL043489.

Patro, P. K., and G. D. Egbert (2008), Regional conductivity structure of Cascadia: Preliminary results from 3D inversion of USArray transportable array magnetotelluric data, *Geophys. Res. Lett.*, *35*, L20311, doi:10.1029/2008GL035326.

Pommier, A., and E. Le Trong (2011), "SIGMELTS": A web portal for electrical conductivity calculations in geosciences, *Comput. Geosci.*, doi:10.1016/j.cageo.2011.01.002, in press.

Pommier, A., F. Gaillard, M. Pichavant, and B. Scaillet (2008), Laboratory measurements of electrical conductivities of hydrous and dry Mt. Vesuvius melts under pressure, *J. Geophys. Res.*, *113*, B05205, doi:10.1029/2007JB005269.

Schmandt, B., and E. Humphreys (2010), Complex subduction and small-scale convection revealed by body-wave tomography of the western United States upper mantle, *Earth Planet. Sci. Lett.*, *297*(3–4), 435–445, doi:10.1016/j.epsl.2010.06.047.

Schutt, D. L., and K. Dueker (2008), Temperature of the plume layer beneath the Yellowstone hotspot, *Geology*, *36*, 623–626, doi:10.1130/G24809A.1.

Schutt, D. L., K. Dueker, and H. Yuan (2008), Crust and upper mantle velocity structure of the Yellowstone hotspot and surroundings, *J. Geophys. Res.*, *113*, B03310, doi:10.1029/2007JB005109.

Smith, R. B., et al. (2009), Geodynamics of the Yellowstone hotspot and mantle plume: Seismic and GPS imaging, kinematics, and mantle flow, *J. Volcanol. Geotherm. Res.*, *188*, 26–56, doi:10.1016/j.jvolgeores.2009.08.020.

Steinberger, B., R. Sutherland, and R. J. O'Connell (2004), Prediction of Emperor-Hawaii seamount locations from a revised model of global plate motion and mantle flow, *Nature*, *430*, 167–173, doi:10.1038/nature02660.

Tikhonov, A. N., and V. Y. Arsenin (1977), *Solution of Ill-Posed Problems*, V. H. Winston, New York.

Waite, G. P., D. L. Schutt, and R. B. Smith (2005), Models of lithosphere and asthenosphere anisotropic structure of the Yellowstone hotspot from shear wave splitting, *J. Geophys. Res.*, *110*, B11304, doi:10.1029/2004JB003501.

Waite, G. P., R. B. Smith, and R. M. Allen (2006), Vp and Vs structure of the Yellowstone hotspot: evidence for an upper mantle plume, *J. Geophys. Res.*, *111*, B04303, doi:10.1029/2005JB003867.

Xue, M., and R. Allen (2010), Mantle structure beneath the western United States and its implications for convection processes, *J. Geophys. Res.*, *115*, B07303, doi:10.1029/2008JB006079.

Yuan, H., and K. Dueker (2005), Teleseismic P-wave tomogram of the Yellowstone plume, *Geophys. Res. Lett.*, *32*, L07304, doi:10.1029/2004GL022056.

Zhdanov, M. S. (2002), *Geophysical Inverse Theory and Regularization Problems*, 609 pp., Elsevier Sci., Amsterdam.
Zhdanov, M. S. (2009), *Geophysical Electromagnetic Theory and Methods*, 848 pp., Elsevier Sci., Amsterdam.
Zhdanov, M. S., A. Green, A. Gribenko, and M. Cuma (2010), Large-scale three-dimensional inversion of Earthscope MT data using the integral equation method, *Izv. Acad. Sci. USSR Phys. Solid Earth*, Engl. Transl., *8*, 27–35.

M. Cuma, M. Green, A. Gribenko, R. B. Smith, and M. S. Zhdanov, Department of Geology and Geophysics, University of Utah, Salt Lake City, UT 84112, USA. (michael.s.zhdanov@gmail.com)